Fusion Neutron-Induced Soft Errors During Long Pulse D-D Plasma Discharges in the WEST Tokamak

Soilihi Moindjie, Daniela Munteanu, Jean-Luc Autran, Martin Dentan, Philippe Moreau, Francis-Pierre Pellissier, Benjamin Santraine, Jérôme Bucalossi, Victor Malherbe, Thomas Thery, et al.

Fusion Neutron-Induced Soft Errors During Long Pulse D-D Plasma Discharges in the WEST Tokamak

S. Moindjie, D. Munteanu, J. L. Autran, M. Dentan, P. Moreau, F. P. Pellissier, B. Santraine, J. Bucalossi, V. Malherbe, T. Thery, G. Gasiot, P. Roche, M. Cecchetto, R. Garcia Alia

***Abstract*— We have performed real-time soft error rate (SER) measurements on bulk 65 nm static random-access memories (SRAMs) during deuterium–deuterium (D-D) plasma operation at W–tungsten– Environment in Steady-state Tokamak (WEST). The present measurement campaign was characterized by the production of several tens of long pulse discharges (~60 s) and by a total neutron fluence (at the level of the circuits under test) up to ~10^9 n.cm^{-2}, improving the error statistics by a factor of more than 6 with respect to the first measurements obtained in 2020. The experimental results demonstrate the occurrence of bursts of single-event upsets (SEUs) during the most efficient shots and 12% of multiple cell upset (MCU) events. Time-resolved data also show that MCUs are preferentially detected in the last part of these long pulses, providing further evidence that higher energy neutrons, initiated by deuterium–tritium (D-T) reactions due to triton burn-up in the D-D plasma, may play a role in the production of MCUs that cannot be attributed in such large proportions to "low energy" neutrons produced in D-D reactions.**

***Index Terms*— Complementary metal-oxide-semiconductor (CMOS), deuterium–deuterium (D-D), deuterium–tritium (D-T), fusion, neutron, real-time experiment, single-event effects (SEEs), soft-error rate (SER), single-event upset (SEU), static random-access memory (SRAM), tokamak, International Thermonuclear Experimental Reactor (ITER), W–tungsten– Environment in Steady-state Tokamak (WEST).**

I. Introduction

THE WEST tokamak [1] is a research device operated by CEA-IRFM and designed to develop the technology necessary for fusion power [2]. WEST serves as a complementary research tool to the International Thermonuclear Experimental Reactor, the ITER project [3], with a focus on testing new materials, exploring new plasma confinement regimes, and developing steady-state operation [4]. While WEST uses deuterium–deuterium (D-D) plasma and ITER will work with deuterium–tritium (D-T) plasma, the research conducted at the WEST tokamak can still provide valuable insights into the behavior of high-temperature plasmas and the development of new materials and technologies for future fusion reactors. D-D reactions will therefore be used during ITER development and commissioning before introducing tritium fuel. Because both D-D and D-T operations produce a high flux of energetic neutrons, creating a residual neutron field outside the reaction chamber [5,6], the electronics for command control and diagnosis of all future fusion devices will be exposed to nuclear radiation and negatively affected by this environment. Investigations are necessary to quantify such radiation effects on electronics devices, circuits and systems in the perspective of qualification procedures and guidelines [7].

In 2020-2021, we conducted the very first real-time soft-error rate (RT-SER) characterization of complementary metal-oxide-semiconductor (CMOS) bulk 65-nm static random-access memories (SRAMs) subjected to fusion neutrons during D-D plasma operation at WEST (C5 campaign) [8]. The test equipment, installed in the experimental hall in the proximity of the tokamak, was irradiated during machine shots ranging from 1 to 18 s in duration. A total of 48 bit flips were detected for a cumulated neutron fluence of 1.43×10^8 n.cm^{-2} at the device level obtained after 1,252 s (0.348 h) of machine operation [8]. The C5 campaign was an initial effort to evaluate neutron-induced single-event upsets (SEUs) in SRAM circuits [9] exposed to the radiation environment near a nuclear fusion device. The aim was to provide early insight into the reliability of ITER electronics, as the machine is scheduled to operate with nuclear plasma in 2035. This approach was similar to previous studies using a nuclear fission reactor as the neutron source, as explained in [10] and [11].

In this work, new real-time SER measurements with the same setup have been performed during the WEST C7 experimental campaign. This latter was characterized by a series of very long pulses (up to 109 s) and very efficient D-D plasma discharges (up to 10^{14} neutrons per shot). This article presents the new experimental results obtained under these conditions, which are characterized by an improved statistics of single-event upset

Manuscript received September 29, 2023. This work was supported in part by EUROfusion Work-Package "Preparation of ITER Operation" (PrIO).

S. Moindjie and D. Munteanu are with Aix-Marseille University and CNRS, IM2NP (UMR 7334), F-13397 Marseille, France.

J.L. Autran is with Aix-Marseille University and CNRS, IM2NP (UMR 7334), F-13397 Marseille, France, and also with Univ. Rennes, CNRS, IPR (UMR 6251), 35 042 Rennes Cedex, France. (e-mail: jean-luc.autran@univ-amu.fr).

M. Dentan, P. Moreau, F.-P. Pellissier, B. Santraine and J. Bucalossi are with IRFM, CEA – Centre de Cadarache, F-13115 Saint-Paul-lez-Durance, France.

V. Malherbe, T. Thery, G. Gasiot and P. Roche are with STMicroelectronics, F-38926 Crolles Cedex, France.

M. Cecchetto and R. Garcia Alia are with CERN, CH-1211 Genève 23, Switzerland.

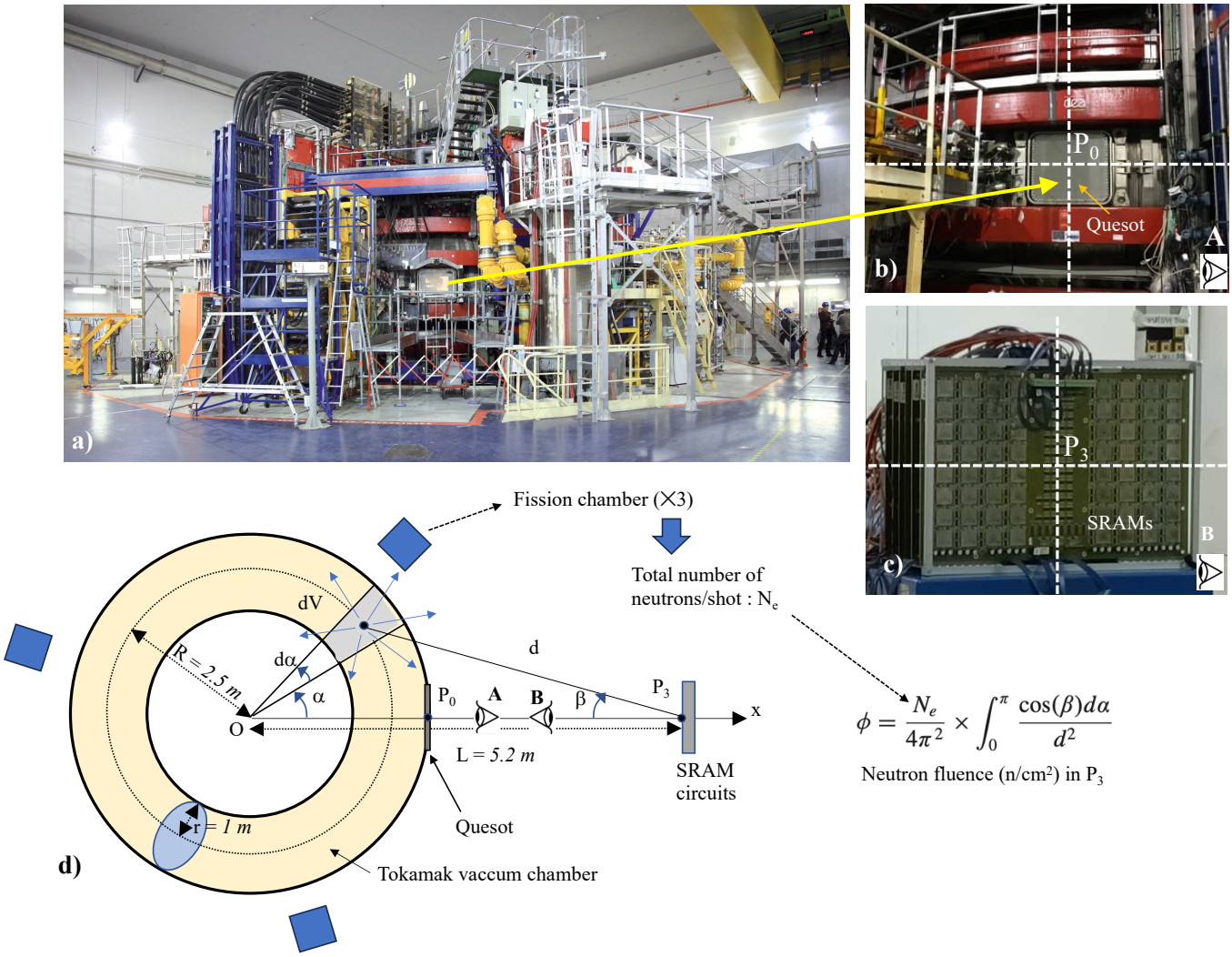

Fig.1. Photographs of the tokamak (a), (b) with the real-time test setup (c) installed at the position P_3 in front of the quesot center P_0 in the tokamak equatorial plan; (d) Schematic top view of the tokamak with the definition of distances. The neutron fluence ϕ at the level of the SRAM circuits under test was estimated from the response of three groups of fission chambers positioned at 120° around the tokamak vacuum chamber. These fission chambers integrate the total number of neutrons N_e produced in the whole tokamak chamber during a machine shot.

(SEU) events, with more than 6 times more bit flips than during the C5 campaign. The article is organized as follows. Experimental details and setups are summarized in Section II. Experimental data obtained during the WEST C7 experimental campaign, including machine pulse characterization and real-time SER measurements, are presented in detail in Section III. Finally, these new results, obtained with the improved statistics, are compared with numerical simulations in Section IV. A detailed discussion of these results in light of the physics and operation of the tokamak is also included.

II. Experimental Details

The RT-SER test setup used for the C5 campaign (see details in [8]) has been reused in the same experimental conditions for the present work at a distance of 5.2 m from the center of the tokamak (position P3 in [8], see Fig. 1). This RT-SER test bench fully complies with all Joint Electron Device Engineering Council (JEDEC) standard JESD89B [12] specifications. We recall here that the setup contains 384 SRAM circuits manufactured by STMicroelectronics in 65 nm bulk CMOS using a borosilicate glass-free process. Each test chip contains 8.5 Mbits of single-port SRAM (without deep-N-well) with a bit cell area of 0.525 µm^2, operated under a nominal core voltage of 1.2 V. This 65nm CMOS bulk SRAM has been extensively characterized under different radiation conditions (neutrons, heavy ions, alpha particles) in previous studies [13-16]. It has also been numerically simulated in 3D using Technology Computer-Aided Design (TCAD) tools. During measurements, the tester scans the full memory array ($384\times8.5\times1024^2 = 3.422$ Gbit) one time every 2.5 s. The SRAM circuits with their upper face oriented toward the center of the machine were placed in the equatorial plane of the tokamak.

The neutron flux monitoring during the machine shots were obtained from the WEST fission chambers (CAF) positioned around the tokamak (Fig. 1). During the C5 campaign, we performed neutron metrology using a commercial DIAMON

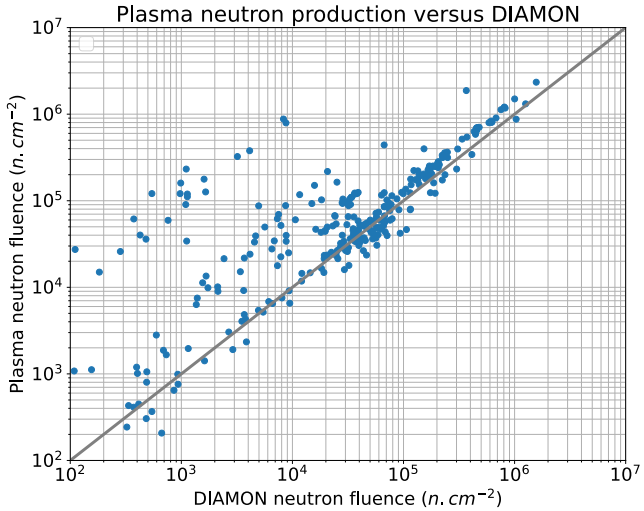

Fig.2. Neutron fluence at the level of the test bench (SRAM circuits) estimated from CAF measurements using the numerical model described in [8] (see Fig. 1) versus direct measurements obtained with the DIAMON spectrometer. During C7 campaign, shot neutron fluences are all above 10^5 n/cm^2 that corresponds to the domain of the curve where CAF versus DIAMON correlation is excellent.

neutron spectrometer [17] to accurately determine the neutron fluence at the level of the test bench. From CAF data and using a numerical model described in [8], we were able to predict the neutron fluence at the level of the test bench with a good agreement with respect to fluences measured using the DIAMON spectrometer.

Fig. 2 shows the correlation between neutron fluences determined from CAF measurements using the numerical model [8] and measured by the DIAMON spectrometer at the level of the exposed circuits. The graph shows that for CAF neutron fluences above a few 10^4 n/cm^2, the correlation between CAF and DIAMON extracted neutron fluences is excellent and in the ratio 1:1. Below a few 10^4 n/cm^2, the correlation is much weaker, or even erroneous, as this area of the distribution clearly corresponds to the shortest machine shots (typically < 3 s), which produced the fewest neutrons during the C5 campaign (see Fig. 6 in [8]). This has a double impact on the flux measurement estimated by DIAMON, since the number of neutrons detected is low and the measurement time (integration time) very short. The spectrum calculated by DIAMON and its integral to obtain the total neutron flux are therefore systematically underestimated in this case. Fortunately, for the C7 campaign, virtually all shot neutron fluences are above 10^5 n/cm^2, corresponding to the region of the curve where the correlation between CAF and DIAMON is precisely 1:1.

III. Experimental Results

The RT-SER test equipment was installed and operated for six weeks during the WEST C7 campaign with a full capacity of 3.422 Gbit. A total of 623 machine shots were produced during this period for a cumulated duration of 12 637 s and a cumulated neutron fluence (at the level of the circuits under test) of 1.21×10^9 n.cm^{-2}. 198 shots were identified to have induced SEUs.

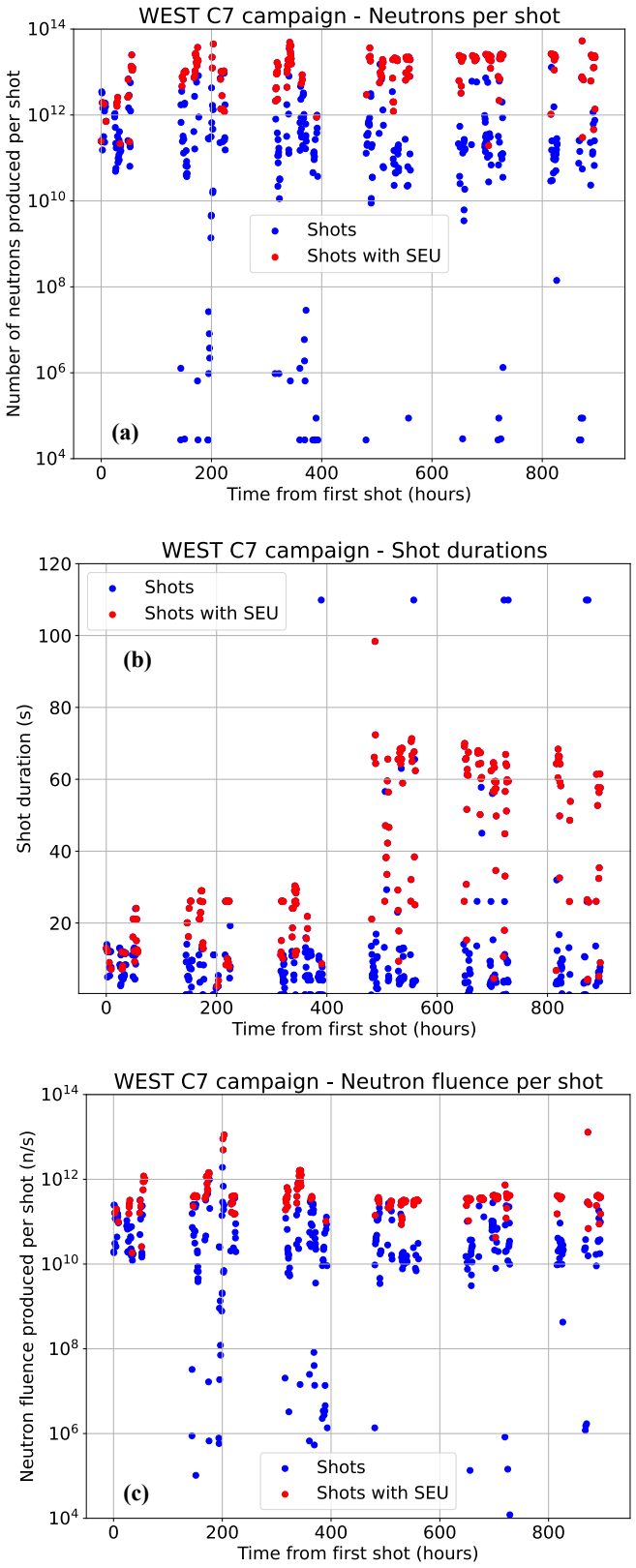

Fig. 3. (a) Distribution of the number of neutrons produced during machine shots, (b) distribution of shot durations (b), and (c) distribution of neutron fluence per shot for all the shots of the WEST C7 campaign (six weeks). Machine shots where SEU events have been detected in coincidence with the neutron flux are shown in red.

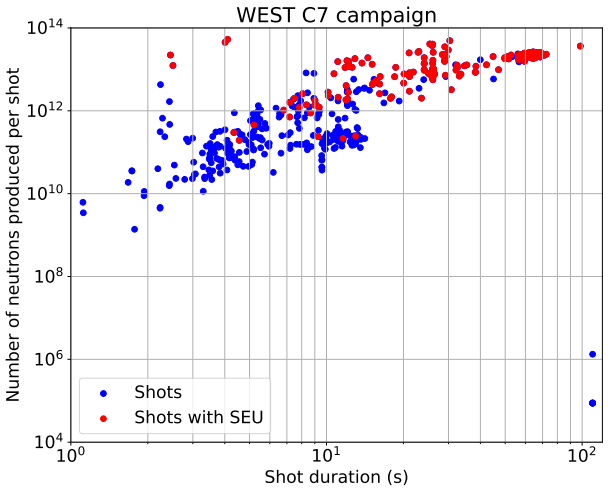

Fig. 4. Distribution of the number of neutrons produced during machine shots versus shot duration for all the shots of the WEST C7 campaign. Machine shots during which SEU events have been detected in coincidence with the neutron flux are indicated in red.

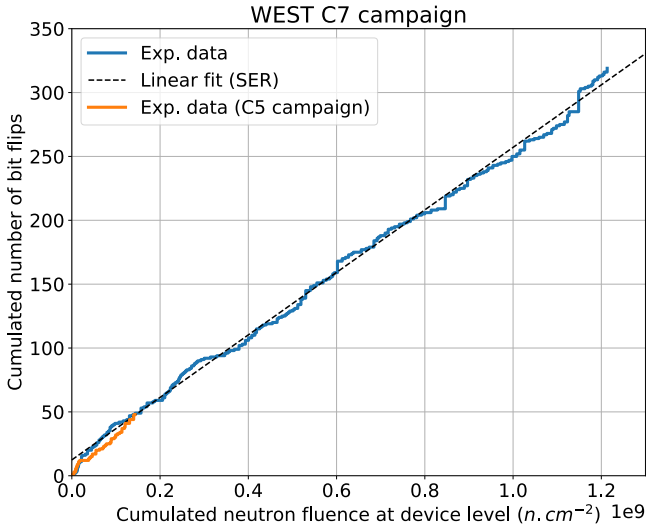

Fig. 5. Bit flip distribution as a function of neutron fluence for all the events detected during the WEST C7 and C5 campaigns. The linear fit corresponds to the extraction of the bit flip SER for data related to C7.

TABLE I
SUMMARY OF C5 AND C7 CAMPAIGNS IN TERMS OF SEUS

	C7 campaign (2023)	C5 campaign (2021)
Maximum shot durations (s)	109	18
Maximum neutrons/shot (tokamak)	5×10^{13}	1×10^{13}
Cumulated neutron fluence ($n.cm^{-2}$) at device level	1.21×10^{9}	1.43×10^{8}
Single Bit Upsets (SBU)	230 (87.1 %)	36 (87.8 %)
MCU events	34 (12.9 %)	5 (12.2 %)
MCU(2)	20	3
MCU(3)	13	2
MCU(>3)	1 MCU(10)	0
Total SBU + MCU events	264	41
Total bit-flips	319	48

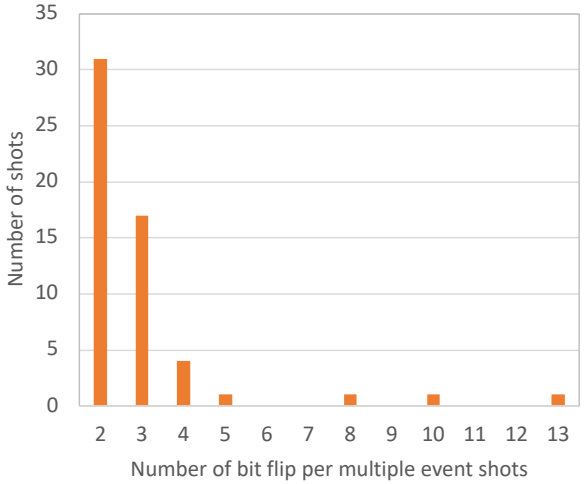

Fig. 6. Histogram of shots characterized by the occurrence at least of 2 bit flips as a function of the number of bit flips detected during the shots. A 2 bit flip occurrence can corresponds to 2 SBUs or 1 MCU(2), a triple bit flip occurrence to 3 SBUs, 1 SBU and 1 MCU(2) or 1 MCU(3), and so on.

Figs. 3 (a), (b) and (c) show the distribution of the number of neutrons produced during shots, the distribution of shot durations, and neutron fluence per shot for all the events, respectively. Machine shots during which SEU events have been detected in coincidence with the neutron flux are indicated in red. Fig. 4 combines data of Figs. 3(a) and 3(b) to show the number of neutrons produced per shot versus shot durations. On the one hand, 130 (90%) on the 144 shots having produced more than 10^{13} neutrons induced SEU(s). On the other hand, only 11 pulses (3.3%) on the 333 having produced less than 10^{12} neutrons induced SEU(s). There is clearly a threshold effect between 10^{12} and 10^{13} neutrons/shot for the production of SEUs.

Concerning the single-bit upset (SBU), multiple cell upset (MCU) and bit flip distributions, a total of 230 SBUs, 20 MCUs of multiplicity 2 [noted MCU(2)], 13 MCUs of multiplicity 3 [MCU(3)] and a single MCU of multiplicity 10 [MCU(10)] have been detected in coincidence with machine shots, representing a total of 319 bit flips.

Two additional events [1 SBU and 1 MCU(2)] were detected during machine shutdown, which roughly corresponds to the test bench's SER in the natural radiation background, taking into account both cosmic rays and traces of alpha particle emitters in circuit materials [14].

Fig. 5 shows the bit flip distribution as a function of the cumulated neutron fluence evaluated at the level of the circuits for all the events detected during the WEST C7 campaign. By comparison, we plotted the 48 bit flips detected during the C5 campaign for a cumulated neutron fluence of 1.43×10^{8} n.cm^{-2} reached at the end of the campaign. The bit flip statistics has been improved by a factor 6.7 in C7 with respect to C5. Such a higher statistics can explain the detection of a rare MCU event with a multiplicity of 10. This MCU is characterized with all adjacent cells in the physical plan of the memory circuit.

Table I compares results obtained during the two campaigns in terms of SBU and MCU ratio. SBUs (resp. MCUs) represent ≈88% (resp. ≈12%) of the detected events, these ratios are

virtually identical for both campaigns, that demonstrates a good repeatability of both irradiation conditions and measurements.

With respect to a reference neutron flux of 20 n·cm^{-2} h^{-1}, the tokamak radiation environment gives an acceleration factor of real-time experiment equal to AF = 2.5×10^{7}. The corresponding bit flip SER in the tokamak radiation environment is equal to n-SER = 4.0×10^{7} Failure In Time (FIT)/Mbit and the bit flip neutron cross section for SRAM in the tokamak field is σ_n = 7.3×10^{-17} cm^2/bit.

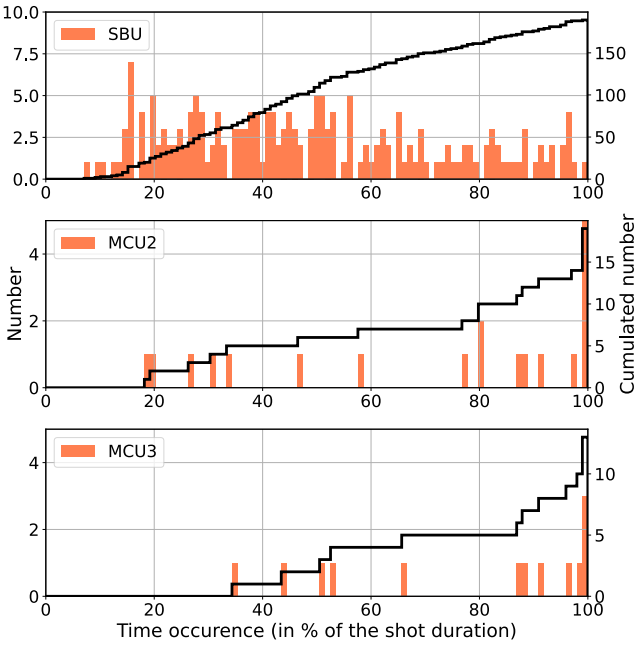

Fig. 7. Time distribution of the occurrence of SBUs and MCU events of multiplicities 2 and ≥3 during the machine shots. A time occurrence of 0 % (resp. 100 %) means that the event occurs at the beginning (resp. at the end) of the machine shot.

Another important and new result obtained in the present work concerns the occurrence of multiple SEU events, that we called “burst events” during the same machine shots. On 198 shots having produced SEUs, 56 shots (among the most efficient in terms of neutron production) resulted in multiple SEU events, i.e., 2 or more SBUs, MCUs or a combination of SBUs and MCUs detected in coincidence with a given shot. Fig. 6 shows the histograms characterizing these burst events in terms of number of bit flips. Double SBU events have been detected during 26 machine shots, triple SBUs five times and quadruple SBU one time.

Due to the short reading/verification cycle of our test bench (as we mentioned, the full memory plan is scanned one time every 2.5 s), the occurrence of multiple events can be resolved in time during a machine shot if the clock of the tester is synchronized with the clock of the tokamak facility. Such a synchronization was done via regular verifications and updating (if necessary) of the PC clock to the time delivered by the tokamak control room. Fig. 7 shows the time distribution of the occurrence of all the SBUs and MCU events of multiplicities 2 and ≥3 during the machine shots. On the horizontal scale, a time occurrence of 0 % (resp. 100 %) means that the event occurs at the beginning (resp. at the end) of the machine shot. Apart from the uncertainty introduced by the memory array reading time, these histograms show a clear difference between the time distribution of SBUs and MCUs during pulses: SBUs are distributed more or less uniformly from the beginning to the end of pulses, while MCUs are predominantly produced during the second half and end of pulses. For the MCU(2), no events are detected in the first 20% of the pulses. Of the 19 MCU(2), only 6 events are detected in the first half of the pulses, and the remaining 13 events in the second half (including 5 at the end of the pulses). For MCU(3), the asymmetry is even more pronounced: no events are detected in the first 30% of the pulses, and of the 14 events detected, only 2 events are detected in the first half of the pulses, while the other 11 events are detected in the second half and near the end (8 over 80% of the pulse duration).

IV. Discussion

These new experimental results obtained during the WEST C7 campaign confirm and bring new elements about the possible role of triton burn-up neutrons in the production of SEUs, a mechanism that was invoked in [8] to explain the occurrence of MCU events in previous experiments. Once the D-D fusion is correctly initiated at the beginning of a machine shot, the concentration of 1 MeV tritons (which are produced in one of the two D-D reactions) rapidly increases in the plasma, making D-T fusion possible. For memory, the D-D fusion follows the two main reactions with equal probability of occurrence:

$$\begin{aligned} D + D &\longrightarrow {}^{3}He(0.82MeV) + n(2.45MeV) \\ D + D &\longrightarrow T(1.01MeV) + p(3.02MeV) \end{aligned} \qquad (1)$$

and D-T fusion follows the main reaction:

$$D + T \longrightarrow {}^{4}_{2}He(3.52MeV) + n(14.07MeV) \qquad (2)$$

This process is known as “triton burn-up” and 14-MeV neutrons produced in D-T reactions that occur in deuterium discharges are called “triton burn-up neutrons” (TBNs) [18].

In our previous work related to the C5 campaign [8], we have shown by both monoenergetic experiments and numerical simulations that such "high energy" D-T neutrons induce much more MCU events in the 65 nm SRAM circuit under test than the primary 2.45 MeV neutrons produced in D-D reactions (in the absence of significant bipolar amplification). On the one hand, we observed 37 MCUs for 4.17×10^{7} n.cm^{-2} of pure 14 MeV neutrons at the Accelerator for Metrology and Neutron applications for external DosimEtry (AMANDE) facility [19] with the same setup. At 2.06 MeV, only a single MCU(2) was observed in a total of 35 events for a neutron fluence of 1.45×10^{7} n.cm^{-2}. On the other hand, always in [8], we reported the modeling and simulation of the 65 nm SRAM exposed to monoenergetic neutrons from 1 MeV to 14 MeV (in steps of 1 MeV) using the Monte Carlo simulation code TIARA [20]. The results of these simulations are shown in Fig. 14 of Ref. [8]. Data show that for neutrons of 3 MeV energy, MCUs represent less than 0.5% of the events, and approximately 9.5% at 14 MeV [8].

In the current work, 34 MCUs events have been detected for a total neutron fluence of 1.21×10^{9} n.cm^{-2} at the device level. The combination of these different experimental and simulation results suggest that "high-energy" neutrons produced in D-T reactions should represent between 2.4 and 3.3% of the total fluence of neutrons (issued from D-D and D-T reactions) estimated at the circuit level. Fig. 8 shows bit flip distributions obtained by numerical simulation [21] for different D-T/D-D neutron fluence ratios ranging from 0% to 5 %. These simulations are based on a multi-Poisson process describing the occurrence of SBUs and MCUs as independent Poisson processes running in parallel with distinct event rates estimated from previous results. Without the contributions of "high-energy" neutrons produced in D-T reactions, there is an evident deficit of bit flips for a cumulated neutron fluence corresponding to that estimated at the circuit level for the C7 campaign (1.21×10^{9} n.cm^{-2}). Increasing the fraction of neutrons issued from D-T reactions causes MCU events to occur. Experimental data is well fitted with the bit flip distribution simulated with a ratio equal to 2.7 %, confirming the raw extraction from MCU statistics.

Nevertheless, this percentage seems slightly higher than the percentage of pure D-T neutrons predicted by tokamak physics (in deuterium plasma discharges in magnetic confinement fusion experiments, the typical triton burnup ratio is 1 % [22]). Triton burnup ratio reported in several studies are typically between 0.5 and 3% [18,22,23]. As explained in [22], the production of 14 MeV neutrons depends on the conditions of 1.01 MeV triton confinement and thermalization. Such a process is easy to achieve in pulses with higher plasma current to reduce triton Larmor radius (i.e., the radius of circular motion of the tritons in the magnetic field developed in the tokamak; it plays a critical role in the behavior of charged particles in the plasma): there is a correlation between the measured D-T/D-D ratio and the plasma current or electron temperature.

Another experimental observation supporting the role of neutrons emitted from D-T reactions in the production of MCUs is the occurrence of these events with a certain delay from the beginning of the pulses and mostly at the end of the pulses, as clearly shown in Fig. 7 for MCU events. This result is consistent with the fact that the triton concentration in the plasma increases from the beginning of a shot [18] (the TBN emission also goes with some delay relative to the birth time of triton). During a pulse, the plasma is enriched with tritium, which favors the production of 14 MeV neutrons, and therefore, the probability of producing MCUs is maximum when the tritium concentration reaches its maximum, i.e., after a certain delay from the beginning of the plasma pulse and rather in its second half. Although the measurements were performed on another tokamak under possibly different operating conditions, Fig. 2 in [23] shows time-resolved profiles of D-D, D-T and D-T/D-D ratios during a D-D discharge at the JET tokamak. The D-T/D-D ratio exhibits a peak at the end of the machine shot, reaching 1.5% for a low plasma current (1.5 MA). Fig. 3 in [23] shows that increasing the plasma current to 6 MA leads to a D-T/D-D ratio larger than 3%.

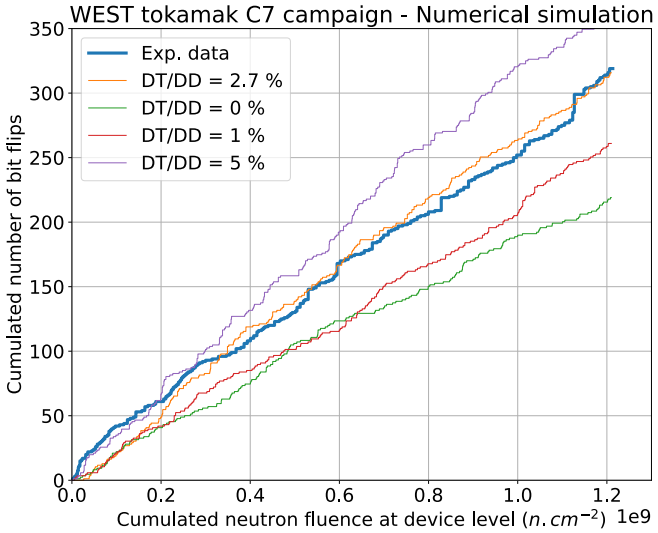

Fig. 8. Comparison between experimental and simulated bit flip distributions for the C7 campaign. Numerical curves have been obtained for different values of the D-T/D-D ratio (0 %, 1 %, 2.7 % and 5 %) and scaled for 3.422 Gbit of SRAM memory.

Qualitatively speaking, similar time evolution and magnitude of this D-T/D-D ratio in the WEST tokamak should explain the occurrences as well as the time distributions of the observed MCUs in the present experiment. A possible contribution of additional "high-energy" photoneutrons in the total neutron fluence at the device level, induced by runaway energetic electrons, may be also invoked to explain these results [24].

V. Conclusion

This work presents experimental results on the RT-SER characterization of bulk 65 nm static random-access memories (SRAMs) exposed to neutrons produced during D-D plasma operation of a tokamak machine at the WEST facility. It significantly improves the previous preliminary experimental results obtained at WEST and goes further in the analysis with a possible link to the physics and operation of the machine. The present measurement campaign at WEST was characterized by the production of several tens of long pulse discharges (~60 s) and by an effective neutron fluence up to ~10^{9} n.cm^{-2} at the device level, improving the error statistics by a factor of more than 6 with respect to the first measurements. Our results highlight the occurrence of bursts of single-event upsets during the most efficient shots and a production of about 12% of multiple-cell upset events. The synchronization of the RT-SER computer clock with the time delivered by the tokamak control room allowed us to show that MCUs are preferentially detected in the second half of the machine pulses, providing further evidence that higher energy neutrons, possibly initiated by D-T reactions due to triton burn-up in the D-D plasma, may play a role in the production of MCUs that cannot be attributed in such large proportions to "low-energy" neutrons produced in D-D reactions.

ACKNOWLEDGMENTS

The authors would like to thank the technical staff of the WEST tokamak facility for their technical support during all the irradiation campaign. This work was supported in part by EUROfusion Work-Package "Preparation of ITER Operation" (PrIO). EUROfusion Consortium is funded by the European Union via the Euratom Research and Training Programme (Grant Agreement No 101052200 — EUROfusion). We would like to express our special thanks to Dr. Xavier Litaudon (CEA/IRFM) for his strong support.

REFERENCES

[1] WEST. (April 06, 2023). W Environment in Steady-State Tokamak. [Online]. Available: http://irfm.cea.fr/en/west/

[2] E. Morse, *Nuclear Fusion*. Cham, Switzerland: Springer, 2018.

[3] ITER. (April 07, 2023). Unlimited Energy. [Online]. Available: http://www.iter.org

[4] J. Bucalossi, M. Missirlian, P. Moreau, F. Samaille, E. Tsitrone, D. van Houtte, T. Batal, C. Bourdelle, M. Chantant, Y. Corre, X. Courtois, L. Delpech, L. Doceul, D. Douai, H. Dougnac, F. Faïsse, C. Fenzi, F. Ferlay, M. Firdaouss, L. Gargiulo, P. Garin, C. Gil, A. Grosman, D. Guilhem, J. Gunn, C. Hernandez, D. Keller, S. Larroque, F. Leroux, M. Lipa, P. Lotte, A. Martinez, O. Meyer, F. Micolon, P. Mollard, E. Nardon, R. Nouailletas, A. Pilia, M. Richou, S. Salasca, and J.M. Travère, "The WEST project: Testing ITER divertor high heat flux component technology in a steady state tokamak environment," *Fusion Eng. Des*., vol. 89, nos. 7–8, pp. 907–912, Oct. 2014.

[5] B. Kos, T. Vasilopoulou, S.W. Mosher, I.A. Kodeli, R.E. Grove, J. Naish, B. Obryk, R. Villari and P. Batistoni, "Analysis of DD, TT and DT Neutron Streaming Experiments with the ADVANTG Code," *EPJ Web Conf.*, 225, 02003, 2020.

[6] J. Wesson, *Tokamaks*, 4th ed. Oxford, U.K.: Oxford Univ. Press, 2011.

[7] M. Dentan, G. Borgese, J. L. Autran, D. Munteanu, S. Moindjie, J. Bucalossi, P. Moreau, F. P. Pellissier, B. Santraine, P. Roche, V. Malherbe, R. Garcia Alia, and M. Cecchetto, "Preliminary Study of Electronics Reliability in ITER Neutron Environment," *Radiation and its Effects on Components and Systems Conference (RADECS) 2022 Proc*., in press ⟨hal-03735989⟩.

[8] J.L. Autran, S. Moindjie, D. Munteanu, M. Dentan, P. Moreau, F. P. Pellissier, J. Bucalossi, G. Borgese, V. Malherbe, T. Thery, G. Gasiot, and P. Roche, "Real-Time Characterization of Neutron-Induced SEUs in Fusion Experiments at WEST Tokamak During D-D Plasma Operation," *IEEE Trans. Nucl. Sci.*, vol. 69, no. 3, pp. 501-511, March 2022.

[9] D. Munteanu and J. L. Autran, "Modeling and simulation of single-event effects in digital devices and ICs," *IEEE Trans. Nucl. Sci.*, vol. 55, no. 4, pp. 1854–1878, Aug. 2008.

[10] A. J. N. Batista, C. Leong, B. Santos, A. Fernandes, A. R. Ramos, J. P. Santos, J. G. Marques, J. P. Teixeira, and B. Gonçalves., "Test results of an ITER relevant FPGA when irradiated with neutrons," in Proc. 4th *Int. Conf. Advancements Nucl. Instrum. Meas. Methods Appl. (ANIMMA)*, Lisbon, Portugal, Apr. 2015, pp. 480–483.

[11] A. J. N. Batista, C. Leong, B. Santos, A. Fernandes, A. R. Ramos, J. P. Santos, J. G. Marques, I. C. Teixeira, J. P. Teixeira, J. Sousa, and B. Gonçalves, "SEU mitigation exploratory tests in a ITER related FPGA," *Fusion Eng. Des.*, vol. 118, pp. 111–116, May 2017.

[12] JEDEC Standard, "Measurement and Reporting of Alpha Particle and Terrestrial Cosmic Ray-Induced Soft Errors in Semiconductor Devices," N° JESD89B, Revision of JESD89A, Sept. 2021.

[13] J. L. Autran, P. Roche, S. Sauze, G. Gasiot, D. Munteanu, P. Loaiza, M. Zampaolo, and J. Borel, "Altitude and underground real-time SER characteri- zation of CMOS 65 nm SRAM," *IEEE Trans. Nucl. Sci.*, vol. 56, no. 4, pp. 2258–2266, Aug. 2009.

[14] J. L. Autran, D. Munteanu, S. Sauze, G. Gasiot, and P. Roche, "Altitude and underground real-time SER testing of SRAMs manufactured in CMOS bulk 130, 65 and 40 nm," in Proc. *IEEE Radiat. Effects Data Workshop (REDW)*, Paris, France, Jul. 2014, pp. 9–16.

[15] J. L. Autran, D. Munteanu, S. Moindjie, T. Saad Saoud, S. Sauze, G. Gasiot, and P. Roche, "ASTEP (2005–2015): Ten years of soft error and atmospheric radiation characterization on the plateau de Bure," *Microelectron. Rel.*, vol. 55, nos. 9–10, pp. 1506–1511, Sept. 2015.

[16] D. Giot, P. Roche, G. Gasiot, J. L. Autran, and R. Harboe-Sorensen, "Heavy ion testing and 3-D simulations of multiple cell upset in 65 nm standard SRAMs," *IEEE Trans. Nucl. Sci.*, vol. 55, no. 4, pp. 2048–2054, Aug. 2008.

[17] A. Pola, D. Rastelli, M. Treccani, S. Pasquato, and D. Bortot, "DIAMON: A portable, real-time and direction-aware neutron spectrometer for field characterization and dosimetry," *Nucl. Instrum. Methods Phys. Res. A, Accel. Spectrom. Detect. Assoc. Equip.*, vol. 969, Art. no. 164078, July 2020.

[18] H. Sjöstrand, G. Gorini, S.Conroy, G. Ericsson, L. Giacomelli, H. Henriksson, A. Hjalmarsson, J.Källne, D. Palma, S. Popovichev, M. Tardocchi, and M.Weiszflog, "Triton burn-up neutron emission in JET low current plasmas," *J. Phys. D: Appl. Phys.*, vol. 41, pp. 129801, May 2008.

[19] AMANDE. (April 07, 2023). Monoenergetic neutron fields, AMANDE facility. [Online]. Available: http://en.irsn.fr/en/research/scientific-tools/experimental-facilities-means/gf-amande-facility/Pages/default.aspx

[20] T. Thery, G. Gasiot, V. Malherbe, J.L. Autran, and P. Roche, "TIARA: Industrial platform for Monte Carlo single-event simulations in planar bulk, FD-SOI, and FinFET," IEEE Trans. Nucl. Sci., vol. 68, no. 5, pp. 603–610, May 2021.

[21] S. Moindjie, J.L. Autran, D. Munteanu, G. Gasiot, and P. Roche, "Multi-Poisson process analysis of real-time soft-error rate measurements in bulk 65 nm and 40 nm SRAMs," *Microelectron. Rel.,* vol. 76-77, pp. 53-57, Sept. 2017.

[22] K. Ogawa, M. Isobe, S. Sangaroon, E. Takada, T. Nakada, S. Murakami, J. Jo, G. Q. Zhong, Yipo Zhang, S. Tamaki, and I. Murata, "Time-resolved secondary triton burnup 14 MeV neutron measurement by a new scintillating fiber detector in middle total neutron emission ranges in deuterium large helical device plasma experiments," *AAPPS Bull.*, vol. 31, pp. 20, Aug. 2021.

[23] G. Nemtsev, V. Amosov, S. Meshchaninov, S. Popovichev, R. Rodionov, and JET Contributors, "Study of the triton-burnup process in different JET scenarios using neutron monitor based on CVD diamond", *Review of Scientific Instruments*, vol. 87, pp. 11D835, Nov. 2016.

[24] B. N. Breizman, P. Aleynikov, E.M. Hollmann, and M. Lehnen, "Physics of runaway electrons in tokamaks," *Nuclear Fusion*, vol. 59, no. 8, pp. 083001, June 2019.